



UNIVERSITÀ DI PARMA

ARCHIVIO DELLA RICERCA

University of Parma Research Repository

Directional and notch effects on the fatigue behavior of as-built DMLS Ti6Al4V

This is the peer reviewed version of the following article:

Original

Directional and notch effects on the fatigue behavior of as-built DMLS Ti6Al4V / Nicoletto, G.. - In: INTERNATIONAL JOURNAL OF FATIGUE. - ISSN 0142-1123. - 106:(2018), pp. 124-131. [10.1016/j.ijfatigue.2017.10.004]

Availability:

This version is available at: 11381/2839270 since: 2021-10-13T15:02:16Z

Publisher:

Elsevier Ltd

Published

DOI:10.1016/j.ijfatigue.2017.10.004

Terms of use:

Anyone can freely access the full text of works made available as "Open Access". Works made available

Publisher copyright

note finali coverpage

(Article begins on next page)

02 May 2026

Elsevier Editorial System(tm) for
International Journal of Fatigue
Manuscript Draft

Manuscript Number: IJFATIGUE-D-17-00536

Title: DIRECTIONAL AND NOTCH EFFECTS ON THE FATIGUE BEHAVIOR OF AS-BUILT
DMLS Ti6Al4V

Article Type: Original Research Paper

Keywords: additive manufacturing, Ti6Al4V, fatigue, notch effect, surface
roughness

Corresponding Author: Professor gianni nicoleto,

Corresponding Author's Institution: Universita di Parma

First Author: gianni nicoleto

Order of Authors: gianni nicoleto

Manuscript Region of Origin: Europe

Covering letter

Title: DIRECTIONAL AND NOTCH EFFECTS ON THE FATIGUE BEHAVIOR OF AS-BUILT DMLS Ti6Al4V

Journal: INTERNATIONAL JOURNAL OF FATIGUE

Dear Editor,

I am here submitting the manuscript entitled: DIRECTIONAL AND NOTCH EFFECTS ON THE FATIGUE BEHAVIOR OF AS-BUILT DMLS Ti6Al4V

for possible publication in the International Journal of Fatigue.

The DMLS acronym stands for Direct Metal Laser Sintering, a proprietary (EOS GmbH Germany) technology belonging to metal Additive Manufacturing realm.

The manuscript presents original results and, in my opinion, draws interesting conclusions on the topic of notch fatigue for Ti6Al4V produced in additive manufacturing. The industrial sectors especially interested are aerospace, biomedical and motorsports.

Best regards

Prof. Gianni Nicoletto

Parma, 2017-08-16

1
2 DIRECTIONAL AND NOTCH EFFECTS ON THE FATIGUE BEHAVIOR
3 OF AS-BUILT DMLS Ti6Al4V
4
5
6
7

8 Gianni Nicoletto
9

10 Dept. of Engineering and Architecture
11

12 University of Parma
13

14 43124 Parma - Italy
15

16 gianni.nicoletto@unipr.it
17
18
19
20
21
22
23
24
25
26
27
28
29
30
31
32
33
34
35
36
37
38
39
40
41
42
43
44
45
46
47
48
49
50
51
52
53
54
55
56
57
58
59
60
61
62
63
64
65

Abstract

1 The metal additive manufacturing technology produces physical components of any geometrical
2 complexity directly from a computer model. Full exploitation of metal AM technology may result in parts
3 that can be lighter in weight, cheaper to produce, and have complex geometries that are difficult or
4 impossible to produce with conventional methods. Two aspects significantly affecting the fatigue behaviour
5 of DMLS Ti6Al4V are investigated: i) the as-built surface condition, which is known to introduce a
6 significant knock-down factor in fatigue with respect to the machined condition, and ii) the presence of a
7 geometrical notch, which affect conventional materials but has not yet been studied in metal AM parts. After
8 the preliminary determination of the reference unnotched fatigue response, the notch fatigue behavior of as-
9 built DMLS Ti6Al4V specimens is determined. Four different notch fatigue factors are estimated including
10 the influence of notch direction with respect to build direction and the up-skin and down-skin notch
11 fabrication condition.
12
13
14
15
16
17
18
19
20
21
22
23
24
25
26
27
28
29

30 Key-words: fatigue, selective laser melting, Ti6Al4V, build direction, notch effect, surface roughness
31
32
33
34
35
36
37
38
39
40
41
42
43
44
45
46
47
48
49
50
51
52
53
54
55
56
57
58
59
60
61
62
63
64
65

1. Introduction

The metal additive manufacturing (AM) technology produces physical components of any geometrical complexity directly from a computer model. Full exploitation of metal AM technology may result in parts that can be lighter in weight, cheaper to produce, and have complex geometries that are difficult or impossible to produce with conventional methods, [1]. Aerospace, biomedical, energy production, motorsports are some of the industries that have been impacted by the rapid evolution of metal AM technology. Here in addition to metal AM, the following acronyms are used: SLM for Selective Laser Melting stressing the use of a laser as energy source and DMLS for Direct Metal Laser Sintering in relation to the commercial AM system used here in practice.

The current qualification or certification procedures of aerospace industry rely on a “building block” concept and a statistical approach based on extensive mechanical test data to quantify uncertainty with respect to material and process variations, [2]. The expensive and time consuming building block design process involves many stages based on physical testing at each stage, starting from material property evaluation testing and ending with full-scale verification testing. While the material behavior of conventional manufactured metal parts is well known, this is not the case for AM-produced components. Therefore, many studies have been published on the link of the metal AM technology and the static mechanical properties, but still limited is the information of the fatigue behavior of AM metals.

Titanium alloys have a key role in aerospace. Structural parts are developed using forging and casting processes because of the excellent strength to weight ratio, high corrosion and temperature resistance etc., [3]. The most widely used and studied Ti-alloy, Ti6Al4V, is playing a key role in the metal AM technology development because all commercial powder-bed-fusion systems can process this alloy for part production. Intensive effort is concentrated in demonstrating the viability of the production and certification of AM Ti6Al4V structural parts.

However, an effective qualification and certification approach requires a good understanding of the large number of machine-to-machine and process parameter variabilities, and their impact on fatigue performance. There are currently more than 100 process parameters reported in the literature, [1], which affect selective laser melt (SLM) material performance, only a few of which are considered and discussed in the literature data. SLM parameters include: layer thickness, laser power, build direction, hatch spacing, scan speed, etc., [4]. The scan strategy used to produce SLM specimens can have a significant influence on attributes, such as the produced residual stresses, [5], or subsurface defect creation, [6,7], which in turn significantly affect fatigue performance for the data presented in the literature is typically not reported. Post fabrication heat treatments of SLM Ti6Al4V have been also investigated and found to be critical for improving the mechanical properties, [8].

The potential for AM to be used for the structural parts of an aircraft is closely related to the possibilities to manufacture complex geometries. While current technology is capable of producing near theoretical density parts without internal defects, a part with a complex geometry will have some areas with rough as-

1 built surfaces, since all surfaces will neither be accessible for machining nor polishing, nor will it be cost
2 efficient to machine all surfaces. Therefore, the combined effect of a rough as-built surface and a geometrical
3 notch needs to be established to enable relevant fatigue predictions for structural parts, [9].
4

5 The as-built fatigue behaviour of SLM Ti6Al4V has been studied in the last few years. Starting from 2014
6 to present several studies investigated the influence of a number factors. Recently ref. [2] provided a critical
7 review of these papers aimed at providing an organized overview of factors and measured influences on
8 fatigue behavior. One of the major challenges is the poor fatigue behaviour of the rough as-built surfaces of
9 AM parts since the fatigue behaviour of AM parts is dominated by the rough surface rather than by internal
10 defects [9]. Surface roughness acts as stress concentrations thus raising the local stress and causing a fatigue
11 crack initiation.
12

13 This contribution is focused on the presentation of original evidence on the notch fatigue behavior of as-
14 built DMLS Ti6Al4V. A special experimental methodology based on the use of miniature specimens is
15 presented and validated against standard specimens produced under the same conditions. The combined
16 effect of a rough as-built surface and a geometrical notch is then presented and discussed in the light of a
17 notch fatigue factor definition. The notch fatigue behavior of SLM metals is not documented in the literature,
18 except for [8]. These notch fatigue results on as-built DMLS Ti6Al4V are therefore used to assess the main
19 findings of this paper.
20
21
22
23
24
25
26
27
28
29
30

31 **2. Approach and experimental details**

32
33
34 In this section the material and process parameters are initially provided, then the original experimental
35 approach based on the use of mini specimens is introduced and the test program described.
36
37

38 *2.1. Material and DMLS process*

39
40 The DMLS process was used on Ti6Al4V ELI alloy powder supplied by EOS GmbH with spherical
41 powder particles and a predominant diameter range from 25 to 45 μm . The fatigue specimens were fabricated
42 using an EOS M 290 system. This system uses an Yb fiber laser unit with a wavelength of 1075 nm with a
43 max laser power of 400 W and layer thickness of 60 μm . The selective laser melting process took place under
44 protective argon atmosphere with a process chamber temperature of 80 $^{\circ}\text{C}$.
45
46
47

48 After fabrication and removal from build plate, all specimens were heat treated in a vacuum furnace as
49 follows: 740 $^{\circ}\text{C}$ for 2 h then slow cooling in vacuum to 530 $^{\circ}\text{C}$ and final cooling to room temperature in
50 Argon atmosphere. This heat treatment reduces residual stresses of the fabrication process to negligible
51 levels.
52
53

54 The microstructure was observed using a light optical microscope Zeiss Axio Observer Z1M on polished
55 and etched (10% HF for 10 s) samples directly cut from the test specimens. The microstructure consists of
56 fine needles of α -phase in β matrix and it was discussed elsewhere, [8, 10]. The material density was
57 measured and is equal 99.7% of the theoretical density.
58
59
60
61
62
63
64
65

Standard tensile specimens produced in the same job of the fatigue specimens were machined and tested and provided the following reference characteristics: ultimate tensile strength UTS = 1176 MPa, yield stress $\sigma_y = 1104$ MPa and elongation to rupture $E\% = 12.9\%$. They are all better than the minimum ASTM requirements for AM Ti6Al4V, namely UTS= 895 MPa and $E\% = 10\%$, [11].

2.2. Fatigue specimen geometry

A characteristic feature of this study is the use of a specially developed specimen geometry (i.e. prismatic, 23 mm in length, 5×5 mm² minimum cross section, 5×7 mm² gross section and lateral semi-circular notch 2 mm in radius) to be subjected to plane cyclic bending loading, [12]. Previous studies demonstrated that this specimen geometry and loading condition result in coherent (i.e. not equal) fatigue data as those obtained using standard rotating bending specimens, [13].

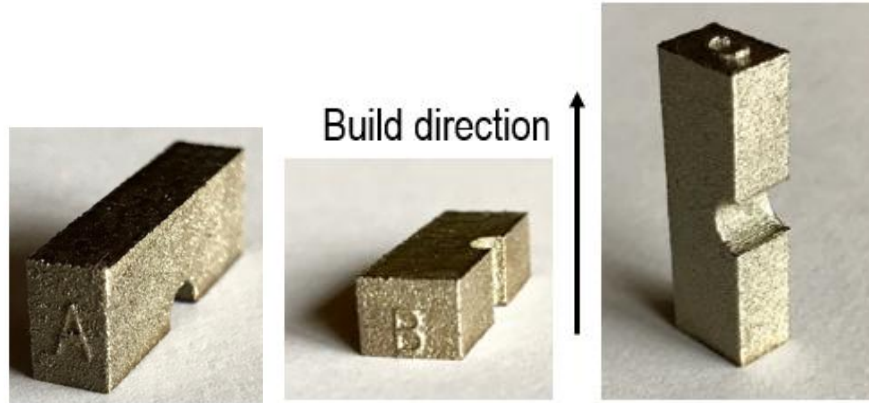
There are several distinct advantages in the use of this test methodology, at least for exploratory study of the fatigue behavior of SLM materials. They are briefly mentioned here as they are exploited in this study.

First, the miniature size involves a drastic reduction of material and production costs, which are a sensitive issue for the fatigue qualification of SLM technology. The estimated reduction in volume is 1/7 with respect to an equivalent rotating bending geometry, Fig. 1, and up to 1/70 of a standard push-pull geometry.



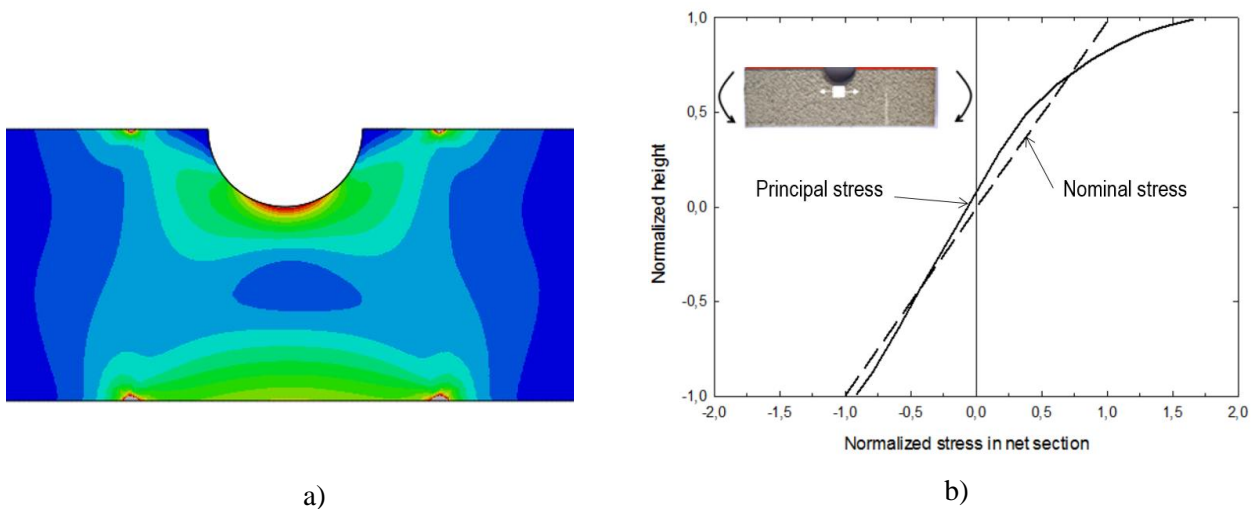
Figure 1 Alternative types of fatigue specimens

Second, these as-built mini specimens can be manufactured with their long axis oriented perpendicular and parallel to the build direction and no support removal required. Fig. 2 schematically shows the positioning on the build plate of individual specimens with three different orientations with respect to the build direction and the respective denomination. The principal longitudinal stress orientation when subjected to bending loading is different for the three specimens of Fig. 2: namely the stress in Type A and Type B specimens is parallel to the layers while it is perpendicular to the layers in Type C specimen. The directionality of the fatigue behavior can be readily investigated using these differently oriented specimens under the same loading condition as previously demonstrated in the investigation of DMLS Ti6Al4V, [13].



14 Figure 2 Definition of specimen type depending on specimen orientations with respect to build direction
15 Type A (left) Type B (center) Type C (right)

16
17
18
19 A third feature is especially relevant for this work: this specimen geometry allows the evaluation of either the
20 unnotched or a specific notched fatigue behavior, with a reduction of time and costs in generating data about
21 the notch fatigue behavior. The results of an elastic finite element study of the stress distribution in the
22 reference minimum cross section of the proposed mini specimens due to the bending loading are given in Fig.
23
24
25 3a. The applied bending load, schematically shown in the inset of Fig. 3b, produces a linear nominal stress
26 distribution with peak tensile stress at the notch root. The elastic stress distribution of Fig. 3 b is non linear
27 and is characterized by a stress concentration factor $K_t = \sigma_{11} / \sigma_n = 1.63$, where σ_{11} is the maximum principal
28 stress and σ_n is the nominal stress due to bending or $\sigma_n = M/W$ where M is applied bending moment and W is
29 the section modulus of the minimum cross-section given by $W = (bxh^2)/6$ with b and h the section thickness
30 and height, respectively. It is worth noting that flat specimen surface, opposite to the notch, is subjected
31 basically to the nominal bending stress, (i.e. $\sigma_{11} / \sigma_n = -0.92$). Therefore, if the orientation of the bending
32 loading shown in Fig. 3 is reversed, the max tensile stress occurs at the flat side and the specimen is
33 substantially subjected a nominal bending stress.
34
35
36
37
38
39
40



59 Figure 3 – a) Elastic stress distribution in the mini specimen under bending b) Normalized principal stress
60 σ_{11} / σ_n due to bending load in the net section of the mini specimen.
61
62
63
64
65

Therefore, selective application of the cyclic load ratio $R = M_{\min}/M_{\max} = 0$ to the specimen results in a fatigue failure originating either on the notch side or on the flat side, as shown in Fig. 4. This feature will be exploited to investigate simultaneously the influence of direction and notch on the fatigue behavior of the as-built SLM material.

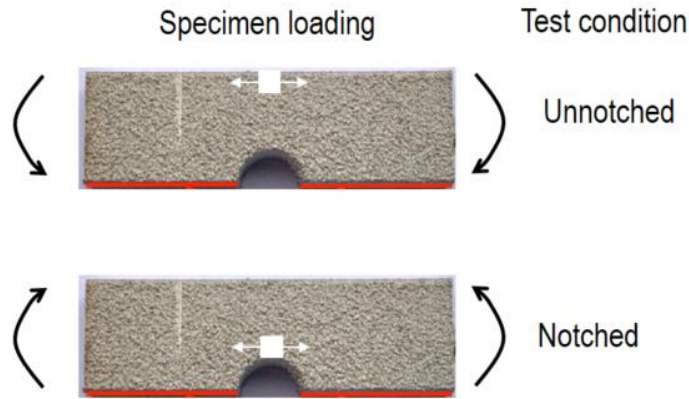


Figure 4 – Different cyclic bending loading under $R=0$ applicable to the mini specimen and corresponding test conditions investigated with the same specimen geometry

2.3. Surface roughness characterization

An important issue of the fatigue behavior of as-built DMLS Ti6Al4V is the relatively high roughness, see [13, 14, 15]. The roughness depends on a combination of raw material quality (powder particle size), additive manufacturing system and processing parameters as reported in [16]. Although machining may result in a smooth surface it is not always a viable approach from the economical and functional standpoints. Besides AM process parameters and powder quality, as-built DMLS surfaces show different morphology in dependence of surface orientation with respect to the build direction. The diagram roughness vs surface orientation of Fig. 5 is taken from a DIN norm, [17].

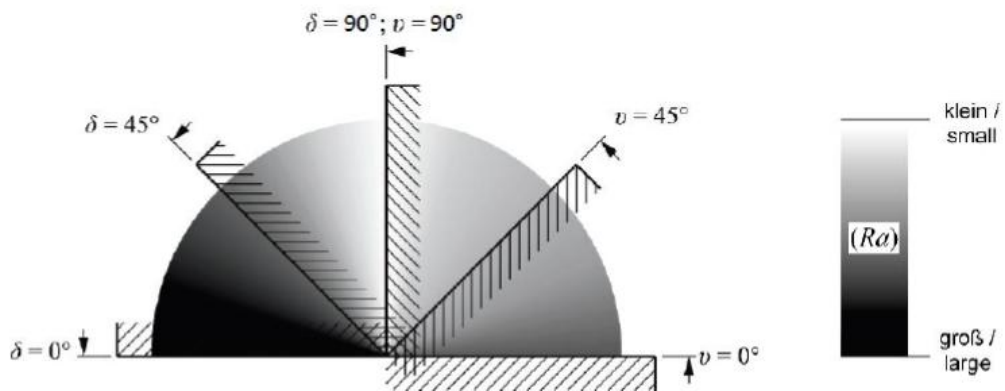


Figure 5 – Relationship between up-skin angle and down-skin angle and roughness R_a for SLM []

1 It uses two angles, namely δ to define a down-skin surface and ν to define an up-skin surface, to map
 2 qualitatively the expected surface roughness (in terms of R_a). Apparently, the surface orientation $\delta = \nu = 90^\circ$
 3 has the lowest roughness, $\delta = 0^\circ$ has the highest roughness and $\nu = 0^\circ$ has an intermediate roughness.
 4

5 In this study both the flat and the notched surfaces are tested in fatigue. Examination of the present
 6 specimen geometry shows that the flat surfaces are characterized by $\delta = \nu = 90^\circ$ in Type B and Type C
 7 specimens and by $\nu = 0^\circ$ in Type A specimens. Surface roughness of the as-built flat surfaces was measured
 8 in the longitudinal direction on a Mitutoyo SJ 210 machine, [10]. The results are summarized in Tab. 1. It is
 9 observed that Type B and Type C specimens have the same roughness, while Type A specimen has a lower
 10 roughness. When checked against the diagram of Fig. 5, the present measurements do not agree with the
 11 predicted values. As the surface roughness of a notch varies from point to point along the profile, it is not
 12 considered here.
 13
 14
 15
 16
 17
 18
 19

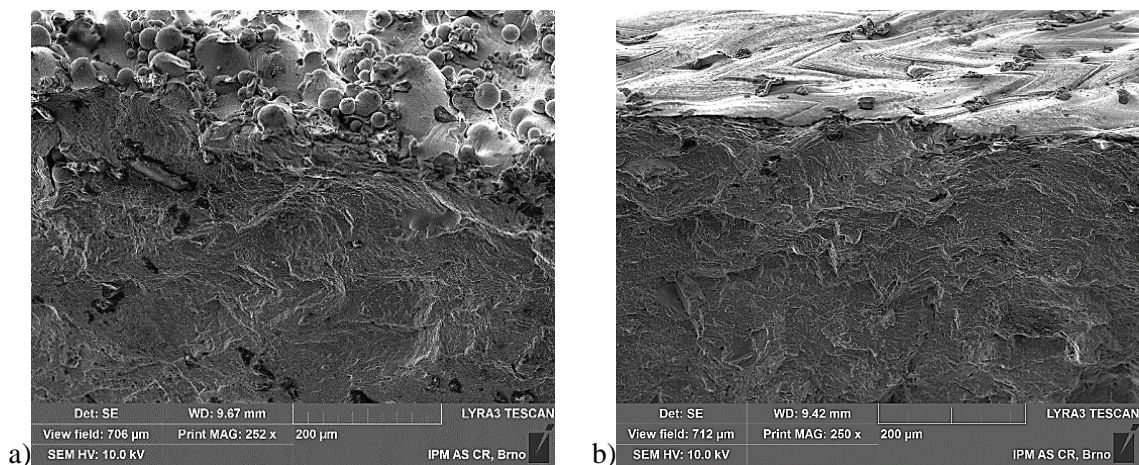
20 Table 1 Surface roughness measured in the longitudinal direction of the flat specimen surface

21

Roughness	Type A	Type B	Type C
Ra [μm]	3.3 ± 0	13.1 ± 0.3	13.4 ± 0.5
Rz [μm]	20.1 ± 3.3	88.8 ± 8.7	80.7 ± 8.2

22
23
24
25
26
27
28

29 A SEM investigation of broken specimens shows the surface characteristics of an as-built surface: Fig. 6a
 30 shows the typical grainy texture due to partly melted powder grains superposed to the smooth melted
 31 material. This kind common to the flat surfaces of Type B and Type C specimens. Type A specimen can be
 32 fabricated according to two opposite (i.e. top or bottom) notch positions. In the case of the flat surface on top
 33 (i.e. $\nu = 0^\circ$), the as-built surface shown in Fig. 6b differs from Fig. 6a. It is characterized by a low roughness
 34 with local shallow notches between neighboring melt strips and limited presence of partially melted particles.
 35 These observations are coherent with measured data of Tab. 1.
 36
 37
 38
 39
 40
 41



58 Figure 6 – SEM micrographs of broken specimens showing: (a) typical as-built surface (i.e. applicable to
 59 test surfaces of Type B and Type C specimens); (b) top surface of Type A specimens.
 60
 61
 62
 63
 64
 65

2.4. Fatigue testing program

The rather lengthy presentation of the experimental methodology of the present study ends with a few more details and a summary of the fatigue testing program. Fatigue experiments were performed under cyclic plane bending on a Schenk type testing machine modified to continuous monitoring of the applied bending load during the test under a fixed displacement range at a frequency of 15 Hz, [12]. Tests were interrupted above 2×10^6 cycles, if specimen did not fail (i.e. run-out).

The cyclic bending moment with $R = 0$ resulted in a nominal tensile stress range $\Delta\sigma = \sigma_{\max}$ on the surface where the crack initiation was desired (i.e. either the flat unnotched surface or the notch root). The test program involved seven sets of mini specimens divided in three groups, one per specimen type, namely two sets of Type C specimens, two sets of Type B specimens and three sets of Type A specimens.

One set for each group was tested so that crack initiation started from the unnotched surface and provided the directional unnotched fatigue response. The second set for Type B and Type C specimens was tested to obtain crack initiation at the notch root providing directional notch fatigue response.

The remaining two sets of Type A specimens were produced in two different ways: in one case the notch was as shown in Fig. 2a (i.e. down-skin fabrication condition without notch support notch because of its small size) and the other case the notch was on the opposite position (i.e. up-skin fabrication condition). Both were tested in fatigue so as to generate fatigue initiation at the notch root. This is possibly the first case where the fabrication condition of a notch is investigated in fatigue.

3. Results and discussion

This section is organized as follows: i) the present material and process are initially qualified in fatigue using standard specimens and data from the literature; ii) the as-built smooth fatigue data obtained from the mini specimens are validated by comparison with standard test results on the same material; iii) the as-built notch fatigue data integrating the directional effect are presented and the directional notch fatigue factors estimated; iv) the present as-built notch fatigue data are compared to the recent notch fatigue data on the same material, [9].

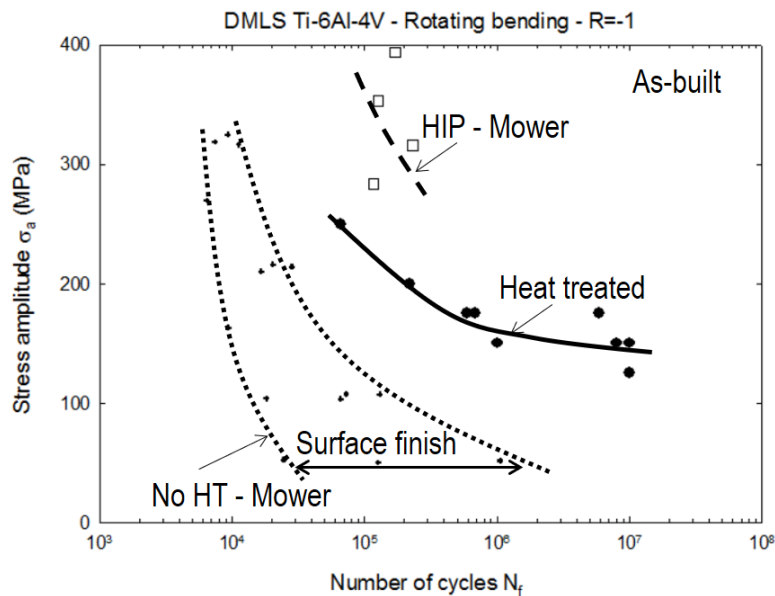
3.1. Reference fatigue behavior of DMLS Ti6Al4V

Preliminarily to the presentation and discussion of the notch fatigue test results, in this section the fatigue behavior of the present DMLS Ti6Al4V after heat treatment and in the as-built surface condition is given and placed in the context of current knowledge as determined from the recent literature. The review of the fatigue behavior of Ti6Al4V, reported in [2], examined the literature and showed the role of heat treatment on performance, of the as-built vs machined surfaces and of the AM Ti6Al4V vs the conventional Ti6Al4V.

Here only the rotating bending condition to generate the test data is considered and shown in Fig. 7, [15]. The absence of a heat treatment results in very poor performance, which cannot be improved simply modifying the surface. Inspection of the broken specimens revealed the presence of critical internal defects

1 due to suboptimal process parameters. Therefore, as-built specimens were subjected to Hot Isostatic Pressing
 2 (HIP) treatment, with an increase in performance visible in Fig. 7. However, the few data presented show a
 3 rapid decrease with stress in performance as the increase in ductility after HIPing helps at low number of
 4 cycles. Recent data on high quality DMLS Ti6Al4V, [9], showed that HIP is not improving the fatigue
 5 performance of as-built specimens because it cannot interfere with the key influence on fatigue of the surface
 6 roughness.
 7
 8
 9

10 The fatigue data of a set of rotating bending specimens produced with the DMSL process and heat
 11 treatment described in the previous section and with as-built surfaces are presented in Fig.7. The trend of
 12 these data defines a reference response that will be used to assess the results obtained with non standard
 13 specimens (i.e. miniature) of Fig. 2.
 14
 15



16
17
18
19
20
21
22
23
24
25
26
27
28
29
30
31
32
33
34
35
36
37
38
39
40
41
42
43
44
45
46
47
48
49
50
51
52
53
54
55
56
57
58
59
60
61
62
63
64
65

Figure 7 – Comparison of rotating bending tests performed on as-built DMLS Ti6Al4V showing the importance of heat treatment, the role of surface finish and of HIP treatment (Mower stands for [15]).

3.2. Directional smooth fatigue behavior of DMLS Ti6Al4V

The fatigue data of all three types of mini specimens tested in the unnotched configuration, (see Fig. 4), are presented in Fig. 8. They represent the reference response for the subsequent discussion of notch effects on fatigue. Fig. 8 shows that the degree of directionality of the fatigue behavior of the present as-built DMSL Ti6Al4V after heat treatment is relatively limited. The qualitative trends outlined are relatively close to one another. A previous study on the same material and process but a low-temperature stress relief heat treatment, [12], resulted in a distinct difference among Type A and Type B specimen directions, on one hand, and the Type C specimens, on the other hand, with the latter showing significantly reduced fatigue strength.

The rotating bending fatigue test results obtained using as-built standard specimens oriented in the build direction, see Fig. 1, and produced using the same process parameters and heat treatment are also plotted in

Fig. 8. An equivalent stress amplitude was defined and used to aptly compare data sets obtained under two different load ratios: rotating bending of standard specimens is characterized by $R = -1$ and cyclic plane bending of mini specimens by $R = 0$. The Haigh equation, [18], was used to convert the stress amplitude σ_a at $R=0$ into an equivalent $R=-1$ stress amplitude $\sigma_{a,eq}$ as follows

$$\sigma_{a,eq} = \sigma_a / (1 - \sigma_m / UTS) \quad (1)$$

where σ_m is the mean stress (equal to stress amplitude) and the ultimate tensile strength $UTS = 1100$ MPa. The choice of a linear dependence of the mean stress on fatigue strength described by Eq. (1) was supported by the results of the study on conventional Ti6Al4V reported in [19].

Inspection of Fig. 8 reveals an appreciable degree of correlation between the reference rotating bending data and the Type C mini specimen data: both share the same direction of loading with respect to the material layered structure as they have the longitudinal axis parallel to build direction. Type A specimens show a slightly improved fatigue behavior at low stresses while Type B specimens at high stresses.

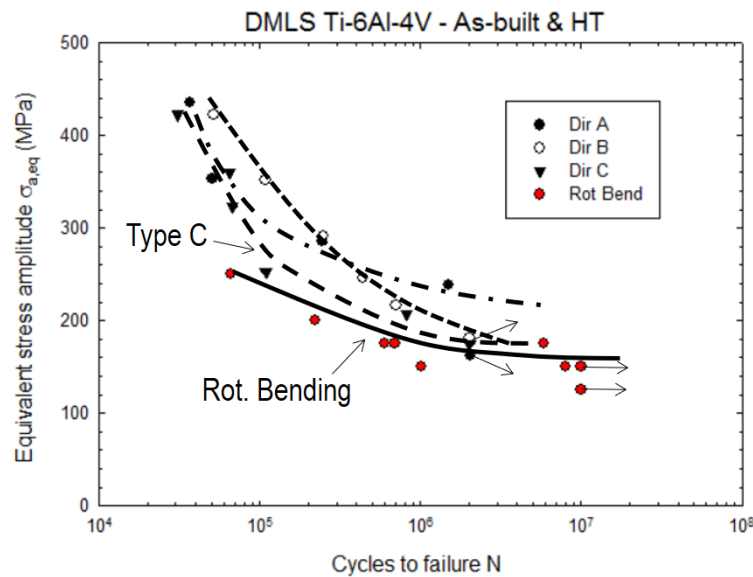


Figure 8 – Comparison of smooth fatigue test results obtained using the three types of mini specimen and a set of rotating bending specimens of DMLS Ti6Al4V after heat treatment and surfaces in the as-built state.

The estimated high cycle fatigue strength of as-built and heat treated DMLS Ti6Al4V is in the range 150 - 180 MPa (as stress amplitude σ_a at $R=-1$) or 300-350 MPa in terms of σ_{max} (at $R=0$). In the literature most fatigue tests are run under tensile cyclic loading at R near zero and data are plotted and discussed in terms of σ_{max} .

Fatigue limits of as-built SLM Ti6Al4V from various studies were compared in [9]. The large spread enlightening the fact that SLM material may have a large variation in performance even for the same type of SLM equipment were used. While that has been definitely true for the initial studies, [2, 14, 15], the fatigue variation among recent studies should reduce because of the on-going refinement of the SLM technology, the

1 experience-based optimization of SLM process parameters and the now established role of post fabrication
 2 heat treatments. Coherently, the present results for as-built DMLS Ti6Al4V agree with recent data published
 3 in [9].

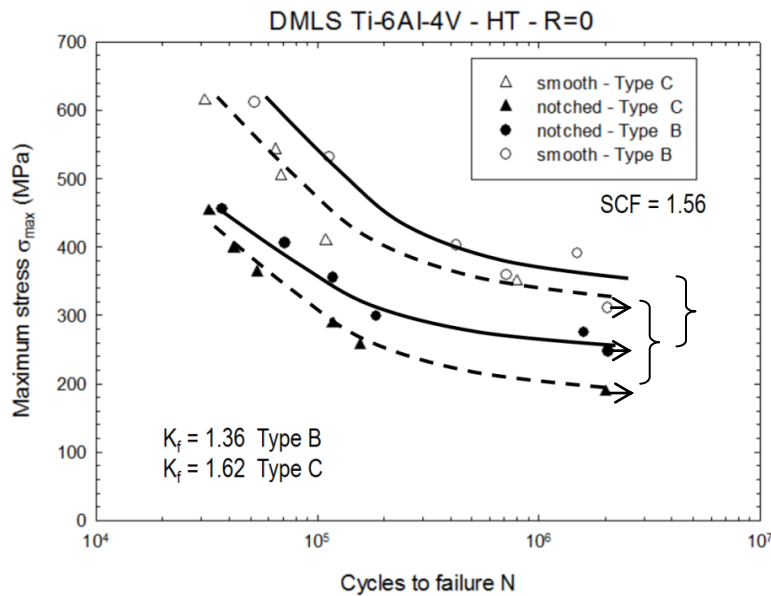
4 Therefore, it believed that the research focus now should be directed to other factors influencing the AM
 5 fatigue performance, such as surface treatments, part geometry, size effects, etc.. The mini specimen
 6 geometry used here may be an efficient alternative to the standard rotating bending configuration, especially
 7 to investigate the influence of SLM process parameters on fatigue.
 8
 9
 10

11
 12 **3.3. Directional notched fatigue behavior**

13
 14 In this section the most significant results of this study are presented. In order to clarify the combined
 15 notch and directional effect on fatigue behavior of as-built DMLS Ti6Al4V, the experimental data are not
 16 inserted in a single plot. Rather, they are divides as follows: Type B and Type C mini specimens are
 17 introduced first; the three sets of Type A mini specimens are presented second.
 18
 19
 20

21 Type B and Type C

22
 23 As-built Type B and Type C mini specimens made of DMLS Ti6Al4V were tested in the two modes
 24 explained in Fig. 4 to quantify the unnotched and notched fatigue behavior and their results are shown in Fig.
 25 9. The data, although limited in number, are well-behaved with a reduced scatter that allows the definition of
 26 individual trends. The lives of Type C specimens are always shorter than those of Type B specimens.
 27
 28
 29
 30



31
 32
 33
 34
 35
 36
 37
 38
 39
 40
 41
 42
 43
 44
 45
 46
 47
 48
 49
 50
 51
 52
 53
 54
 55
 56
 57
 58
 59
 60
 61
 62
 63
 64
 65

Figure 9 Notch fatigue behavior of two types of as-built & heat treated DMLS Ti-6Al-4V specimens:
 broken lines: Type C, continuous line: Type B (load ratio R=0; $K_t=1.56$).

Estimates of the fatigue notch factor K_f for the two fabrication directions are obtained from the experimental trends of Fig. 9 as follows. Adopting the classical definition of K_f as the ratio of the smooth fatigue strength and notch fatigue strength, see [18], Type B $K_{f,B}$, or $K_{f,B}$, and Type C $K_{f,C}$, or $K_{f,C}$, are determined using the respective unnotched and notched responses of Fig 9. Thus, $K_{f,C} = 1.63$ and $K_{f,B} = 1.36$,

respectively. These are possibly the first results of this kind where the influence of the notch surface quality and of the specimen orientation (i.e. parallel and perpendicular to build direction) on fatigue is quantified. When compared to the theoretical $K_t=1.63$ of the present notch geometry, the two experimental K_f , although not too different, show directionality, i.e. SLM technology-dependent.

Type A

The three sets of as-built DMLS Ti6Al4V mini specimens were tested in fatigue under a load ratio $R=0$ with the aim of investigating the up-skin/down-skin fabrication condition of the notch. Type A+ and Type A- are associated to different notch position during fabrication: Type A+ is associated to up-skin notch while Type A- is associated to down-skin notch.

The test results in terms of max nominal bending stress vs number of cycles are plotted in Fig. 10. The fatigue data appear well-behaved with a reduced scatter. The up-skin fabrication condition is associated to a slightly better fatigue behavior than the down-skin condition. Although not surprising, it is possibly the first published evidence of this factor on notch fatigue behavior.

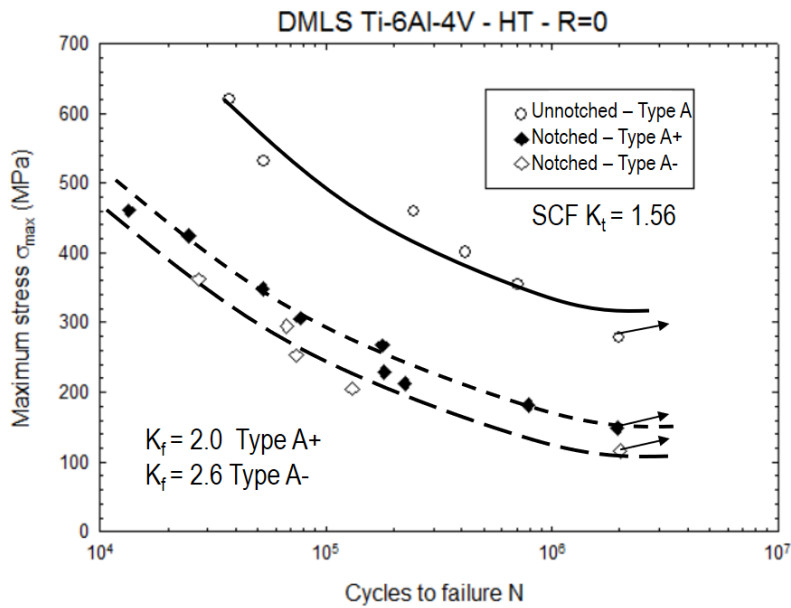


Figure 10 Notch fatigue behavior of as-built & heat treated DMLS Ti-6Al-4V Type A specimens subjected to cyclic plane bending (load ratio $R=0$; $K_t=1.63$).

The trends defined in Fig. 10 allow the experimental determination of an effective notch factor K_f of the two notched configurations Type A+ and Type A- using the unnotched response of Type A as the reference. Type A+ configuration is characterized by $K_{f,A+} = 2.0$ and the Type A- configuration by $K_{f,A-} = 2.6$.

Interestingly, both K_f values are larger than the theoretical K_t value of the notch geometry, in contradiction with classical results for fatigue tests in conventional materials, [18]. A possible motivation is in the difference between the smooth theoretical geometry used in K_t calculation and the two contributions to the effective surface quality of the present SLM notches: i) the surface roughness, which may depend on the up-

skin vs down-skin notch generation, see Fig. 5, and ii) the step-wise generation of the theoretically semicircular Type A notch geometry. This specific aspect is currently under investigation.

3.4. Comparison with the literature

While the published data for smooth fatigue behavior of DMLS Ti6Al4V can be found in the literature, the notch fatigue behavior is absent except for the recently published data of [9], which is therefore important reference for the present study. The fatigue properties of as-built Ti6Al4V under cyclic tension with $R = 0.1$ were investigated in [9]. Both the selective laser melting and electron beam (EB) melting technologies were considered but only SLM data are used here. Analogously to the present rotating bending specimens, tensile specimen axis was oriented parallel to the build direction. That orientation is also the same of the Type C mini specimens tested here. Tensile cylindrical bars with a V-notch geometry and a notch root of 0.85 mm radius was used. The resulting theoretical stress concentration factor was computed as $K_t = 2.5$. The total length of tensile specimens was 80 mm, therefore compatible in terms of material usage with the present rotating bending specimens of Fig. 1.

The fatigue notch factor, K_f , in [9] was defined as the ratio of the fatigue strength of the smooth and polished conventional Ti6Al4V and fatigue strength of the as-built notched DMLS Ti6Al4V. Differently from the present work, the role of geometry and technology was combined in a unique factor in [9]. The combined fatigue notch factor $K_f = 6.15$ was computed for the SLM process and $K_f = 6.64$ for EB process.

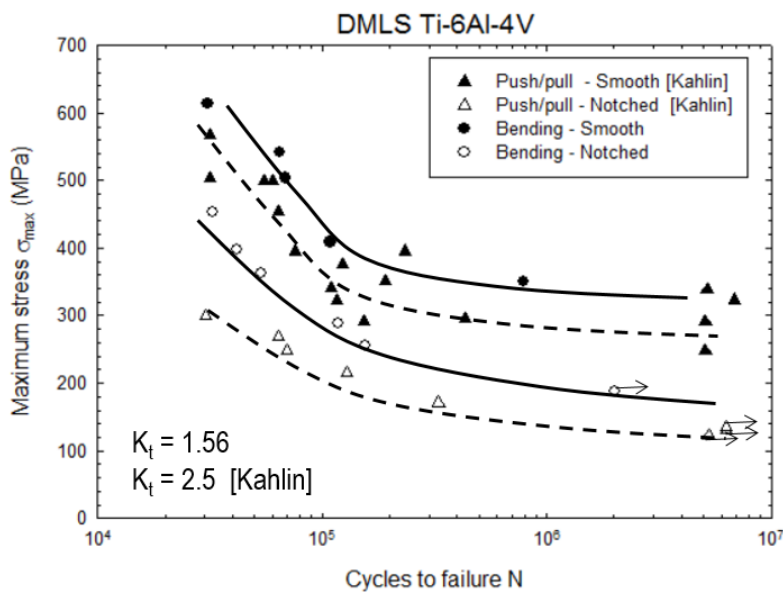


Figure 11 – Comparison of as-built smooth and notched fatigue test results for present Type C mini specimens in cyclic bending and Kahlin’s specimens in cyclic tension. Material is heat treated DMLS Ti6Al4V (Kahlin 2017).

To exploit this limited experimental evidence on the notch fatigue behavior of SLM Ti6Al4V, the cyclic tension data for smooth as-built specimens and notched as-built specimens tested at $R=0.1$ of [8] are plotted

1
2
3
4
5
6
7
8
9
10
11
12
13
14
15
16
17
18
19
20
21
22
23
24
25
26
27
28
29
30
31
32
33
34
35
36
37
38
39
40
41
42
43
44
45
46
47
48
49
50
51
52
53
54
55
56
57
58
59
60
61
62
63
64
65

in Fig. 11 together with the present Type C as-built smooth and notched plane bending data tested at R=0. While no mean stress correction needs to be introduced in the plot (σ_{\max} -N), the type of loading (bending vs. tension) is expected to play a significant role, [19]. Inspection of Fig. 11 reveals the following: the cyclic bending loading is associated to longer lives than cyclic tension, the severe $K_t = 2.5$ geometry of [9] results in shorter lives than the mild $K_t = 1.56$ of Type C mini specimens. According to the definition of K_f given in a previous section of this contribution, the SCF $K_t = 1.63$ of the mini specimens is associated to $K_{f,C} = 1.63$ and the $K_t = 2.5$ of notched bars in tension is associated to $K_f = 2.5$. Apparently, the notch effect in fatigue is directly connected to the stress concentration factor. Although these initial results are based on still limited evidence, more effort in this direction is welcome.

4. Conclusions

Original evidence on the notch fatigue behavior of as-built DMLS Ti6Al4V obtained in this study has provided new understanding of the complex but technically relevant issue of structural design of AM parts. The following conclusions are reached:

- The smooth as-built fatigue strength of heat treated DMLS Ti6Al4V is determined to be about 300 MPa in agreement with recent literature findings;
- The experimental methodology based on the use of miniature specimens was validated against a standard test geometry. It can be efficiently used to investigate the fatigue response of SLM alloys;
- The notch as-built fatigue strength of heat treated DMLS Ti6Al4V is directional: here four different notch fatigue factors are estimated by comparing smooth and notched fatigue strength of seven sets of specimens.
- Up-skin and down-skin notch fabrications have a different impact on fatigue strength.
- The present notch fatigue factors for as-built DMLS Ti6Al4V are coherent with recently published values for the same material.
- To the author's best knowledge this experimental evidence appears for the first time in the literature.

Acknowledgements

Specimen fabrication by the company BEAM-IT, Fornovo Taro, Italy (www.beam-it.eu) is acknowledged with thanks.

References

- [1] Bandyopadhyay, A., Bose, A. Additive manufacturing: Additive manufacturing technologies of metals using powder-based technology. Taylor & Francis Group: Boca Raton, (2016).
- [2] Li P., D. H. Warner, A. Fatemi, and N. Phan, "Critical assessment of the fatigue performance of additively manufactured Ti-6Al-4V and perspective for future research," Int. J. Fatigue, vol. 85, (2016), pp. 130–143.

- 1
2
3
4
5
6
7
8
9
10
11
12
13
14
15
16
17
18
19
20
21
22
23
24
25
26
27
28
29
30
31
32
33
34
35
36
37
38
39
40
41
42
43
44
45
46
47
48
49
50
51
52
53
54
55
56
57
58
59
60
61
62
63
64
65
- [3] Lütjering G., Williams J.C., A. Gysler A., Microstructure and mechanical properties of titanium alloys. Titanium: Springer Science and Business Media, (2007).
 - [4] Rafi H. K., N. V. Karthik, H. Gong, T. L. Starr, B. E. Stucker, “Microstructures and mechanical properties of Ti6Al4V parts fabricated by selective laser melting and electron beam melting”, *Jou of Materials Engineering and Performance*, 22, (2013) 3872-3883.
 - [5] Shiomi, M., Osakada, K., Nakamura, K., Yamashita, T., Abe, F. Residual stress within metallic model made by selective laser melting process. *Journal of the CIRP Annals - Manufacturing Technology*, vol. 53, no. 1, (2004) pp. 195-198.
 - [6] Simonelli, M., Tse, Y.Y., Tuck, C. Further understanding of Ti-6Al-4V selective laser melting using texture analysis. In *23rd Annual International Solid Freeform Fabrication Symposium (2012)* pp. 480-491.
 - [7] Wycisk E., C. Emmelmann, S. Siddique, and F. Walther, “High Cycle Fatigue (HCF) Performance of Ti-6Al-4V Alloy Processed by Selective Laser Melting,” *Adv. Mater. Res.*, vol. 816–817, (2013), pp. 134–139.
 - [8] Vrancken B., Thijs L., Kruth J.P., Van Humbeeck J., Heat treatment of Ti6Al4V produced by Selective Laser Melting: Microstructure and Mechanical properties, *Journal of Alloys and Compounds*, (2012). 541(0): p. 177-185.
 - [9] Kahlin M., H. Ansell, J.J. Moverare, Fatigue behaviour of notched additive manufactured Ti6Al4V with as-built surfaces, *International Journal of Fatigue* 101 (2017) 51–60
 - [10] Konečná R., G. Nicoletto, S. Fintová, M. Frkáň, As-built surface layer characterization and fatigue behavior of DMLS Ti6Al4V, *Proceedings FMDM3, Lecco 2017*, in press
 - [11] ASTM F2924-14, Standard Specification for Additive Manufacturing Titanium-6 Aluminum-4 Vanadium with Powder Bed Fusion, ASTM International, West Conshohocken, PA, www.astm.org (2014)
 - [12] Nicoletto G. Anisotropic high cycle fatigue behavior of Ti-6Al-4V obtained by powder bed laser fusion. *International Journal of Fatigue*, vol. 94, (2014), pp. 255-262.
 - [13] Bača A., R. Konečná, G. Nicoletto, L. Kunz, Influence of build direction on the fatigue behaviour of Ti6Al4V alloy produced by direct metal laser sintering, *Materials Today: Proceedings* 3 921-924 (2016).
 - [14] Edwards P., Ramulu M. Fatigue performance evaluation of selective laser melted Ti–6Al–4V, *Mater. Sci. Eng. A*, (2014), A598, 327–337
 - [15] Mower T. M., M. J. Long, “Mechanical behavior of additive manufactured, powder-bed laser-fused materials”. *Materials Science and Engineering*, A651 (2016), pp.198-213.
 - [16] Gong, H., Rafi, K., Starr, T., Stucker, B. The effects of processing parameters on defect regularity in Ti-6Al-4V parts fabricated by selective laser melting and electron beam melting. In *24th Annual International Solid Freeform Fabrication Symposium*. (2013), pp. 424-439.

1
2
3
4
5
6
7
8
9
10
11
12
13
14
15
16
17
18
19
20
21
22
23
24
25
26
27
28
29
30
31
32
33
34
35
36
37
38
39
40
41
42
43
44
45
46
47
48
49
50
51
52
53
54
55
56
57
58
59
60
61
62
63
64
65

[17] VDI-Guidline 3405 Part 3 Dec 2015, Additive Manufacturing Processes, Rapid Manufacturing – Design Rules for Part Production using Laser Sintering and Laser Beam Melting (2015)

[18] Juvinall R., Marshek K.M., Fundamentals of Machine Component Design, . New York: John Wiley, (2012)

[19] Nicholas T., High Cycle Fatigue: A Mechanics of Materials Perspective, Elsevier (2006)